27. Preston, S. T., "Vapor-Liquid Equilibrium Constants from Gas Chromatography Data," Proceedings of NGAA (April, 22-24, 1959).
28. Price, A. Roy, and Riki Kobayashi, *J. Chem. Eng. Data*, 4, No. 1, p. 40 (1959).
29. Rangel, Enrique T., M.S. thesis, Rice University, Houston, Texas (Sept., 1956).
30. Sage, B. H., and W. N. Lacey, "Thermodynamic Properties of the Lighter Paraffin Hydrocarbons and Nitrogen," Monograph on API proj. 37, American Petroleum Institute, New York (1950).
31. Stalkup, F. I., Ph.D. thesis, Rice University, Houston, Texas (Aug., 1961).
32. ———, and H. A. Deans, *A.I.Ch.E. Journal*, 9, 118 (1963).
33. Stalkup, F. I., and Riki Kobayashi, *ibid.*, p. 121.
34. Stoddart, C. T. H., and P. H. Evertt, *Trans. Faraday Soc.*, 57, 746 (1961).
35. VanDeemter, J. J., F. J. Zuiderweg, and A. Klinkenberg, *Chem. Eng. Sci.*, 5, 271 (1956).
36. Wolf, Frank, Humble Oil and Refining Company, Houston, Texas, Private communication.

Manuscript received February 10, 1964; revision received September 22, 1964; paper accepted September 23, 1964.

An Experimental Investigation of Air Bubble Motion in a Turbulent Water Stream

JAMES L. L. BAKER and BEI T. CHAO

University of Illinois, Urbana, Illinois

The motion of individual air bubbles in a water stream flowing turbulently in a 4 in. × 4 in. vertical conduit is investigated by photographic means. The bulk water velocity ranges from 40.8 to 267 cm./sec., corresponding to a system Reynolds number range of 48,600 to 386,000. Both tap and demineralized water were used at or near room temperatures. Air bubbles range from 0.038 to 0.70 cm. in equivalent radius and the corresponding bubble Reynolds number based on relative velocity ranges from 58 to 4,500.

The results indicated that the bubble relative velocity in a turbulent water stream is similar to the rise velocity of single bubbles through a quiescent liquid. It was found to be practically independent of the system Reynolds number for bubbles having an equivalent radius above 0.3 cm. Large fluctuations in the bubble velocities were noted in all cases. The drag coefficient is, in general, lower for the demineralized water tests than for tap water when the bubble Reynolds number is below 2,000. Above this value, a mergence of the drag coefficients for all tests occur with a peak of approximately 2.0 at a bubble Reynolds number of 3,000, which is lower than the nonflow value of 2.6.

The behavior of bubble motion in a turbulent stream of liquid plays an important role in predicting the characteristics of a boiling reactor system. It also finds its importance in many physical and chemical processes involving mass, momentum, and heat transfer between the liquid and gaseous phase.

Although a great deal of effort has been spent by many investigators in different countries to gain an understanding of the behavior of bubble motion in calm liquids, information on the velocity, drag, and shape is practically nonexistent when the bubble is moving in a turbulent stream (*1*).

The motion of air bubbles in calm liquids has been studied both experimentally and theoretically during the past six decades. Early experiments performed by Allen (*2*) showed that for small air bubbles rising in water and in aniline, good agreement was found with Stokes law when the bubble Reynolds number was less than 2. Miyagi (*3*) studied the motion of single air bubbles in water over a radius range of 0.025 to 0.4 cm. His data on terminal velocity indicated a maximum at a bubble radius of approximately 0.15 cm., followed by a slight drop up to bubble radius of 0.3 cm. Larger bubbles exhibited a terminal velocity independent of bubble radius. Davies and Taylor (*4*) measured the shape and rate of rise of extremely large spherical cap-shaped air bubbles in water

J. L. L. Baker is at present at the Argonne National Laboratory, Argonne, Illinois.

and in nitrobenzene and found that the terminal velocity increased as the square root of the equivalent bubble radius. Peebles and Garber (5) gave a concise summary of the experimental findings of many investigators and also reported results of their own. Haberman and Morton (6) conducted extensive investigations on the drag and shape of air bubbles arising in various liquids. Included in their report and a paper on the same subject are two comprehensive bibliographies on bubble motion up to 1956. More recent bibliographies have been prepared by Bloomfield et al. (7) and by Monod (8). It is indicated that bubble motion is a complex phenomenon even in quiescent liquids, and it involves an interplay of viscous, inertial gravity, and interfacial forces. Reference (1) includes a comprehensive survey of past theoretical studies.

This paper presents the results of an investigation of the behavior of the motion of individual air bubbles rising in turbulent water flowing upward in a vertical plastic test column of 4 in. sq. cross section under the following conditions:

1. Demineralized and tap water at system Reynolds number range of 48,000 to 386,000. The corresponding range of bulk water velocity is 40.8 cm./sec. (1.34 ft./sec.) to 267 cm./sec. (8.75 ft./sec.).

2. The individual tests were isothermal with overall range of temperatures of 21.1° (69°F.) to 36.7°C. (98°F.).

3. Air bubbles range in equivalent radius of 0.038 to 0.70 cm.

4. The Reynolds number based upon the bubble relative velocity and equivalent diameter is 58 to 4,500.

Table 1 lists the relevant properties of the tap and demineralized water used in the investigation. Test run T-2* was conducted at a lower water temperature but at an identical flow rate as test T-2 in order to ascertain the effect of temperature and to investigate the influence of parent-satellite interaction on bubble velocities.

DIMENSIONLESS PARAMETERS

Dimensional analysis has played an important role in the reduction of experimental data related to bubble motion. A survey and examination of the published literature on the subject revealed that some of the proposed correlations were in effect only a statement of a definition connecting the several dimensionless groups. An account of such misleading presentation has been given elsewhere (1). The many group formulations can usually be reduced to a combination of the following four groups with the occasional supplementation of density and viscosity ratios for two-component systems. These groups are: the Reynolds number, the Weber number, the Froude number, and the drag coefficient.

TABLE 1. SYSTEM PROPERTIES

Test run	Temperature, °C.	Density, g./cc.	Interfacial tension, σ dynes/cm.	Viscosity, μ centipoise	System Reynolds number, N_{Re_s}
T-1	27.2	0.996	71.3	0.85	48,600
T-2	26.1	0.996	71.5	0.87	86,650
T-2*	20.6	0.997	72.4	0.99	76,300
T-3	27.8	0.996	71.2	0.84	124,600
D-1	30.0	0.995	70.9	0.80	51,500
D-2	30.0	0.995	70.9	0.80	94,100
D-3	29.4	0.995	71.0	0.81	131,000
D-4	36.7	0.992	69.8	0.70	299,000
D-5	36.7	0.992	69.8	0.70	386,000

Two Reynolds numbers are required for the air-water system used in the investigation. They are the system Reynolds number and the relative bubble Reynolds number as defined by

$$N_{Re_s} = \frac{\rho L_o V_{w,\text{mean}}}{\mu} \tag{1}$$

and

$$N_{Re_{b,r}} = \frac{\rho D_{eq} V_{b,r}}{\mu} = \frac{\rho D_{eq} (V_b - V_{w,l})}{\mu} \tag{2}$$

It is to be noted that the presence of a single air bubble has a negligible effect on the bulk water velocity. Thus, the latter is employed in the definition for the system Reynolds number.

The Weber number based on the relative velocity and the equivalent diameter is given by

$$N_{We_{b,r}} = \frac{\rho V^2_{b,r} D_{eq}}{\sigma} \tag{3}$$

The drag coefficient for steady motion is

$$\overline{C_D} = \frac{4}{3} \frac{\Delta\rho}{\rho} \frac{g D_{eq}}{V^2_{b,r}} = \frac{4}{3} \frac{\Delta\rho}{\rho} \frac{1}{N_{Fr_{b,r}}} \tag{4}$$

For the case of an air bubble rising in water at atmospheric pressure, the ratio of the density difference to the density $\Delta\rho/\rho$ is very closely unity.

The product of the Weber number and the drag coefficient is

$$\overline{C_D} \cdot N_{We} = \frac{4}{3} \frac{\Delta\rho\, g\, D^2_{eq}}{\sigma} \tag{5}$$

which represents the ratio of the buoyancy force to the interfacial force. The dimensionless grouping $\frac{\Delta\rho\, g\, D^2_{eq}}{\sigma}$ in the present application is known as the Eötvös number N_{Eo}, as suggested by Harmathy (9). Other investigators (10, 11, 12) have also directly and indirectly employed N_{Eo} in the correlation of data.

There is another group which has appeared, though not always explicitly, in the literature (5, 9, 13). It is

$$\frac{N_{We}}{\overline{C_D}} = \frac{3}{4} \frac{\rho^2 V^4}{g \sigma \Delta\rho} = \frac{3}{4} \frac{\rho}{\Delta\rho} N_{We} N_{Fr} \tag{6}$$

which, upon rearrangement, gives

$$V = \left[\frac{g \sigma \Delta\rho}{\rho^2}\right]^{1/4} \left[\frac{4}{3} \frac{N_{We}}{\overline{C_D}}\right]^{1/4} \tag{7}$$

The dimensional grouping in the first bracket has been employed in reference 5 as a correlation coordinate. Misleading statements have appeared in the interpretation of results. Readers are referred to (1) for further discussion.

EXPERIMENTATION

The circulating water loop is shown in Figure 1. The centrifugal pump, item 8, was capable of delivering a range

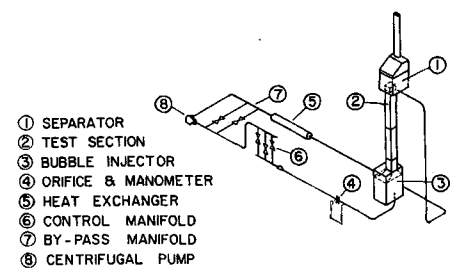

Fig. 1. Schematic of the circulating water loop.

of bulk water velocities in the test section from 40.8 cm. (1.34 ft./sec.) to 270 cm./sec. (8.75 ft./sec). A concentric tube heat exchanger, item 5, provided temperature control. An aluminum tank with a 4-in. stand pipe open to atmosphere, item 1, served the important purpose of removing the air bubbles. The bubbles were generated from an oil free air supply and injected through a guarded slot into the enlarged plastic section, item 3. The provision of the enlarged section was found necessary to avoid bubble breakup when ejected from the wake region of the bubble disseminator at high water flow rates. A series of screens and straighteners were employed to promote a flat water velocity profile. The bulk water flow rate was obtained by calibrating a sharp edged orifice installed in the discharge line from the pump.

The test section, item 2, consisted of four foot long plastic sections with walls of ¾ in. thickness; the inside dimensions were 4 in. × 4 in. (10.16 by 10.16 cm.). The outlet from the enlarged plastic section had three curved transition walls and one straight wall for acceleration smoothing of the water into the test section. All of the test work was carried out in the upper portion of the test unit.

Local water velocity (temporal mean) profiles were obtained by employing a probe unit consisting of two total head traverses mounted in ball joints in opposite plastic walls of a simulated test section, and six wall static pressure taps located at the same level as the total pressure probe tips which extended 2 in. below the center line of the ball joints. These probes were connected across an inverted U-tube manometer. A semicircular platform provided a calibrated location setting for the probes. In general, over two hundred data points were taken for a single flow setting. The results were employed to obtain a topographical map of the water velocity at the cross section and were plotted in terms of the ratio of the local water velocity to the maximum water velocity. They were then graphically integrated to obtain the average to maximum ratio. One such plot is shown in Figure 2 for a bulk water velocity of 266 cm./sec. The average to maximum water velocity ranged from 0.814 to 0.832 and therefore could be considered relatively constant for the entire flow range.

The specific gravity of the manometer fluids and of the water in the test loop were measured by using a constant volume picnometer and a beam balance. A tensionmeter was employed to obtain the surface tension of the tap and demineralized water.

Bubble velocities were evaluated from photographs taken with multiflash exposure. Figure 3 is one of several hundreds of such photographs obtained in the investigation. The bubble shown had an equivalent radius of 0.142 cm. and was rising in tap water flowing at a bulk velocity of 40.8 cm./sec. (1.34 ft./sec.) and at a temperature of 27.7°C. (82°F.). Two electronic strobotacs connected in series supplied the required lighting with flash durations of 3 μsec. or less. A front-faced aluminum-deposited mirror was set at 45 deg. to the test section to provide the second plane of view. Other details

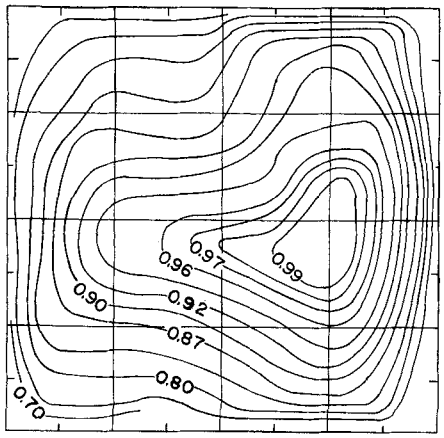

Fig. 2. A topographical map of water velocity in the test section. Numerals represent the ratio of local velocity to the maximum.

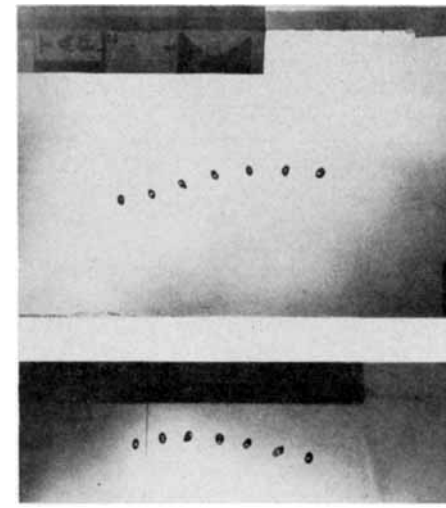

Fig. 3. Individual air bubble motion as revealed by multiflash exposure. (The two views were taken in perpendicular directions.)

and the associated optical corrections are described in the Appendix of reference *1*.

An estimation of the uncertain factors introduced in the determination of bubble relative velocity indicated a maximum error of 3% (based on local water velocity) for the spherical bubbles and 7% for the ellipsoidal and spherical cap bubbles.

RESULTS

Relative Bubble Velocity

The relative bubble velocity obtained for various flow rates and bubble sizes is not quite comparable to the so-called *terminal* velocity of a bubble rising in a quiescent liquid. The usual connotation of the terminal velocity used in the majority of the nonflow investigations is that of an average vertical velocity of the bubble relative to the quiescent fluid determined over a distance such that any cyclic effects in the velocity are repeated many times. In those investigations where high-speed photography was used, such as by Haberman and Morton (6), a short interval was employed in which the velocity was determined to be constant. The relative bubble velocity obtained in the turbulent flow tests was measured over a portion of a cycle for a majority of the cases. It was based upon several incremental average bubble velocities over a short vertical travel of about 6 in. As pointed out by Nicklin (*14*), a distinction must be made as to which portion of the liquid is used as a reference. In these turbulent flow results, the water velocity employed is that of the local

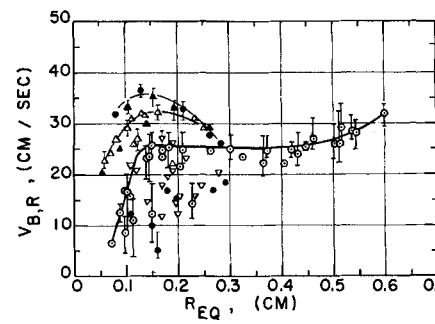

Fig. 4. Variation of bubble relative velocity with equivalent radius. Demineralized water.

△ D-1 Re_s = 51,500
⊙ D-2 94,100
• D-4 Re_s = 299,000
▽ D-3 131,000
▲ D-5 386,000

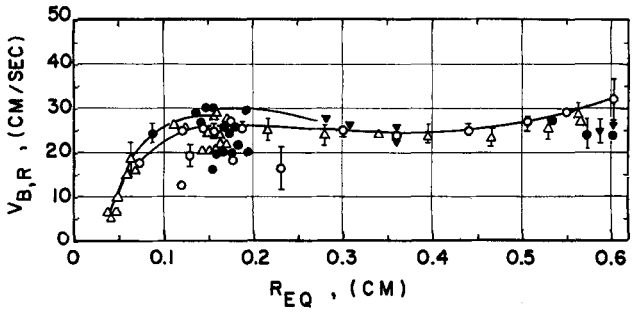

Fig. 5. Variation of bubble relative velocity with equivalent radius. Demineralized water.

△ T-1	Re_S = 48,600	▼ T-2*	Re_S = 76,300
○ T-2	86,650	• T-3	124,600

water velocity obtained from the velocity probe measurements.

In order to eliminate the effect of the large velocity gradients near the wall, the results reported herein were obtained from a 2 in. × 2 in. core region. Original data and enlarged reduced velocity profiles are on file at the University of Illinois. The velocity gradient in the horizontal plane is less than 0.04 cm./sec./cm./unit velocity in this core region. Examination of successive bubble locations did not reveal any preference for the bubble to follow a constant local water velocity contour or to move normal to it. In addition, the relative velocity showed no systematic variation with changes in horizontal location within the core.

Figures 4 and 5 show the variation of individual bubble relative velocities as a function of the equivalent radius. In general, five to six measurements were made for a single bubble to determine the average. It was found that some bubbles possessed a low relative velocity which could be ascribed to the previous history of the bubble. These bubbles were found to have entered the core from a region near the wall.

The fluctuation of the relative velocity about the average is approximately 5 cm./sec. which remains fairly constant over the entire range of bubble sizes. Unfortunately, the random errors due to measurement and the actual bubble velocity fluctuations cannot be separated. The observed constancy of the magnitude of the fluctuation would indicate that the bubble motion is actually varying to a greater degree for the smaller sizes since the deviations in measurements are greater for the larger bubbles.

For bubble diameter less than 0.3 cm., the relative velocity tends to vary in a nonsystematic manner with the various flow rates. For larger sizes, the relative velocity remains relatively constant at approximately 25 to 27 cm./sec. until an equivalent radius of 0.45 cm. is reached beyond which it slowly increases. For larger bubbles, the relative velocities are higher than the corresponding nonflow values. For the small bubbles, the data are less conclusive but the difference is generally small. However, there was one run for which a sharp drop in relative velocity was noted for radii below 0.14 cm. for reasons unknown at present. The range over which the relative bubble velocity remains constant corresponds to an Eötvös number range of approximately 4 to 9. In this range, the ratio of the Weber number to the drag coefficient is a constant. Harmathy (9) indicated that the corresponding Eötvös number range was 1 to 13 for bubbles in quiescent fluids.

In general, the relative velocity of air bubbles in upward concurrent, turbulent flow water is slightly higher than the terminal velocity in quiescent water; the exception occurs at extremely small bubble sizes.

Bubble Interaction

Several parent-satellite bubbles were formed in the course of this study, and the large interaction between them prompted the inclusion of Figure 6 in which the parents are indicated by "Q" and the satellites by "SAT Q". Both satellites SAT Q5 and SAT Q6 exhibited relative velocities far in excess of individual bubbles of similar size and, at the same time, showed very large velocity fluctuations. For the parent bubble Q8, there were two satellites, labeled A and B in Figure 6. The A satellite was closer to the parent than the B satellite. Although the number of bubble interaction cases is limited in this study, the large scale fluctuations in relative velocity are apparent. Not only does the wake region of the parent affect the satellite, but the presence of the satellite produces an effect on the parent also. It was found that as one bubble (parent or satellite) accelerated, the other decelerated.

The effect of bubble interaction for the nonflow case has been reported by Garner and Hammerton (15). The bubble terminal velocity for streams of rising bubbles in water is greater than that of single, individual bubbles of the same diameter.

Drag Coefficient

The drag coefficient-Reynolds number plot in Figure 7 is based on the equivalent diameter and relative velocity Reynolds number. The system Reynolds number is employed as a parameter. Included are the rigid sphere curve and the results of Haberman and Morton (6) for single air bubbles rising in calm, filtered water.

All the data, with the exception of one test (D-2), indicate a drag coefficient which is lower than that of the rigid sphere for Reynolds numbers below 800. A minimum in the drag coefficient occurs at Reynolds numbers between 500 and 800. The minimums for the nonflow cases occur at slightly lower values. The general trend of all drag coefficients shows a rapid increase for Reynolds number exceeding 800. There appears to be very little difference in the values of drag coefficient for all runs above a Reynolds number of 2,000 A tendency to peak occurs in the neighborhood of $N_{Reb,r}$ = 3,000 at a value lower than the drag in calm water.

In general, the drag coefficients for the demineralized water exhibit lower values than the tap water when the bubble Reynolds number is below 2,000, with the exception of two tests for which the data fall within the rather narrow spread of the tap water results. The shape of the bubbles for these two tests did not vary from the other three demineralized water runs as may be seen in Figure 9. The fact that the bubble aspect ratio data for these two

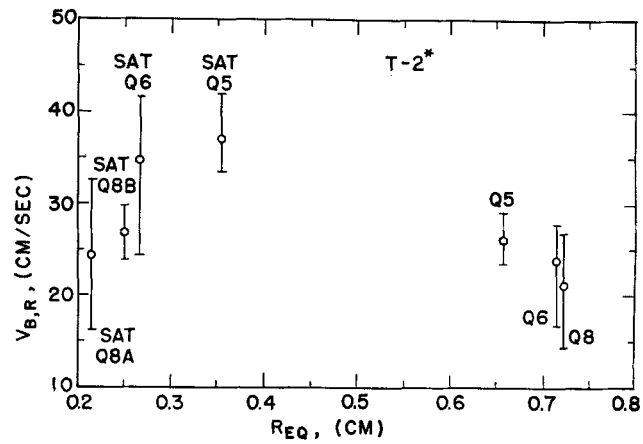

Fig. 6. Large bubble velocity fluctuations due to parent-satellite interaction.

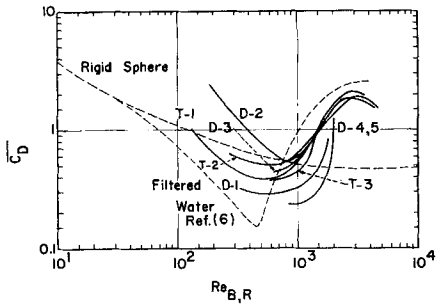

Fig. 7. Variation of bubble drag coefficient with Reynolds number based on relative velocity.

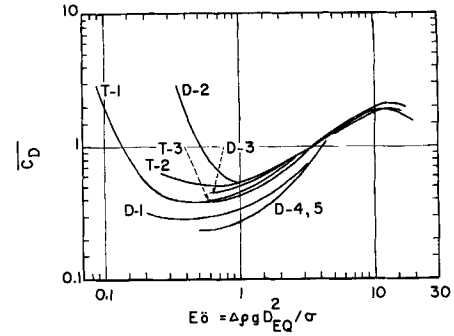

Fig. 8. Bubble drag coefficient as a function of Eötvös number.

tests are not in the tap water region tends to indicate that no contamination was introduced into these tests. Since the aspect ratio is smaller for the demineralized water tests than for the tap water at the same equivalent radius, the drag coefficient becomes lower for the former owing to a smaller projected area in the direction of flow. In addition, for an equivalent radius of 0.35 cm. or larger, the bubble aspect ratio data cease to exhibit a distinction between the two sets of data (see Figure 9). This observation coincides with the fact that the drag coefficient curves tend to merge at large Reynolds numbers.

A plot of the drag coefficient vs. the Eötvös number ($= \frac{3}{4} N_{We} \bar{C}_D$) is shown in Figure 8. This plot illustrates the buoyancy to inertia force ratio as a function of the ratio of the buoyancy to surface force. The drag coefficients tend to merge for Eövtös number greater than 5 (which corresponds to an equivalent radius of 0.3 cm.). It is seen that a peak value occurs at an Eötvös number between 12 and 15. At small Eötvös numbers the drag coefficient curves take different courses, but no systematic variation with system Reynolds number can be noted.

Bubble Trajectory and Shape

In calm water, three general categories of motion have been observed in accordance with the rise path of the bubbles; rectilinear, helical, and cycloidal. The rectilinear motion occurs for small bubbles up to an approximate maximum equivalent radius of 0.06 cm.; however, the reported transition size varies among different investigators (*5, 15*). The ellipsoidal bubbles exhibit a helical motion up to an equivalent radius of approximately 0.3 cm. Above this value the motion is described again as rectilinear in pure liquids with no surface-active agent present. In the presence of a contaminant, the motion is cycloidal in nature; that is there are two stall points in a cycle. Very large bubbles assume the shape of a spherical cap. They appear to have a rectilinear motion in quiescent liquid of large extent.

During the course of the present study, both rectilinear and helical motions were noted. It was difficult to identify the cycloidal motion, since it might appear to be helical when only a portion of the cycle was viewed. The period of the cycle was of the same order as that for quiescent water. Thus, the increase of the absolute bubble velocity at high system Reynolds numbers produced a greater vertical translation during a given cycle and limited the observation of successive cycles.

It has been indicated by many investigations that the major axis of ellipsoidal bubbles remains nearly perpendicular to the direction of motion during the rise in a quiescent fluid. A similar observation cannot be made for the rise of ellipsoidal bubbles in a vertical turbulent stream. The fluctuation from oblate to prolate shape with a period of about one-twentieth of a second at flow velocities of 74 cm./sec. has been observed. It is suggested that the appearance of this large oscillation is due to the combined influence of the velocity gradient in the water and the over-ride of the bubble's attempt to reach an equilibrium shape. Bubbles rising with helical motion in the turbulent flow field tend to increase in amplitude and frequency as the size increases, until a maximum amplitude occurs in a region around an equivalent radius of approximately 0.14 cm. The shape of the bubble in this region is nearly ellipsoidal. With increasing radius, the amplitude subsides and the surface of the bubble tends to form ripples, while deep undulations in the upper surface can be noted at about an equivalent radius of 0.3 cm. A transition to a much smoother surface occurs at an equivalent radius above 0.5 cm., and the bubbles tend toward the spherical cap type although there is large oscillation in the major dimensions. The upward motion of these bubbles appears to be nearly rectilinear. Very small bubbles are very nearly spherical, and they remain so over the entire test range of water flow.

The large cyclic variation in the shape of the bubble as it rises in the spacially nonuniform velocity field of the turbulent flow in the test section would indicate that the induced or apparent mass of the bubble changes and that the upward velocity would be altered locally. It has been pointed out by Birkhoff and Zarantonello (*16*) that the conditions required for the determination of the induced mass are dependent upon the geometry of the free and fixed boundaries and on the direction of translational acceleration. Thus, local turbulent eddies could readily alter the translational acceleration and thereby affect the local velocity. However, the change in form drag due to the change in shape and the possible variation in the separation of flow around the bubble as its shape alters could average out over an interval of time which is long as compared with the characteristic period of such variation.

The ratio of the major axis to the minor axis of ellipsoidal bubbles rising in quiescent water was shown by Rosenberg (*17*) to increase from a value of unity at an equivalent radius of 0.04 cm. to a value of approximately 2.7 at 0.35 cm. and to remain constant for values up to 0.53 cm. Furthermore, a constant diameter-to-height ratio of 4.02 was obtained for spherical caps in the equivalent radius range of 1 to 3 cm. The bubbles in the intermediate size range varied in shape to such a large degree that no specific value was assigned. Harmathy (*9*) plotted the ratio of major to minor axis as a function of Eötvös number in which there was a nearly linear increase in this ratio for the Eötvös number range of 1 to 15 for both liquid-liquid and air-liquid systems. The very large scatter exhibited in his plot was attributed to shape oscillation.

In Figure 9, the ratio of the major to minor axis is shown for both the demineralized and tap water results as a function of the equivalent radius. The data employed in this plot correspond to the maximum aspect ratio for

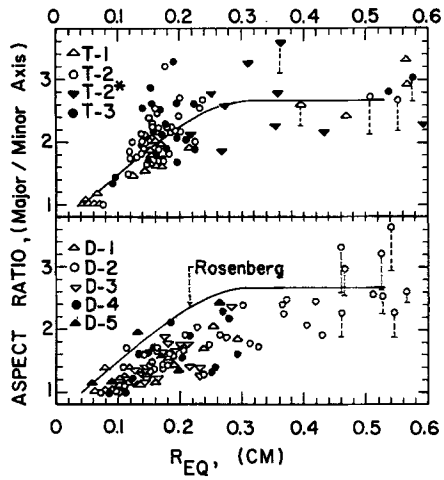

Fig. 9. Bubble deformation as a function of equivalent radius. (Upper figure for tap water, lower figure for demineralized water.)

a bubble which has one of its axes parallel to the film planes. Thus, the value plotted does not necessarily represent the actual maximum. The higher values for a given size would be more representative of the data than the lower values, since a slight tilt of the bubble would result in a lower aspect ratio. Several points have a dashed connection between the upper and lower value for a general ellipsoidal shaped bubble and thereby represent the variation in the bubble shape in a direction normal to flow. The curve given by Rosenberg (*17*) is included for comparison. The demineralized water data fall either on or below the curve for equivalent radii below 0.46 cm. The tap water data are in general above or slightly below the curve up to an equivalent radius of 0.36 cm. Both sets of data tend to merge beyond an equivalent radius of 0.35 cm. For bubble sizes below 0.1 cm., the aspect ratio is again merged since they tend to be spherical. Thus, there appears to be a region from approximately 0.1 to 0.35 cm. equivalent radius in which the tap and demineralized water data are distinctly different. Since the measured surface tension of the tap and of the demineralized water do not differ to any significant degree, the difference in the shape parameter could possibly be ascribed to either a difference in surface charge of the bubble in the two media or to a surface tension change which is not observable in the static determinations. The appearance of a dynamic surface tension which is lower than the static surface tension (as in the tensiometer test) has been indicated in the literature; the more recent work is that of Roll (*18*). An examination of the aspect ratio data shows that the system Reynolds number has no apparent effect.

Fluctuations in the major axis of bubbles larger than 0.35 cm. equivalent radius are generally in the order of 30%. The variation in the major axes in the two views is also approximately 30% as the bubble contracts and expands. The aspect ratio values for the larger bubbles were not included in Figure 9, since no representative value could be obtained owing to the shape fluctuations. Average values of the aspect ratio for large bubbles are greater than the 2.7 which was indicated by Rosenberg, and the maximum values could be as high as 4. No distinction could be made between the tap and demineralized water for the large bubbles.

ACKNOWLEDGMENT

The authors wish to express their sincere appreciation of the financial support of the U. S. Atomic Energy Commission under Cooperative Research Contract No. AT(11-1)-1069, and to Dr. Michael Petrick of the Argonne National Laboratory for calling attention to this problem.

NOTATION

A = flow area $= L_o^2$
D_{eq} = diameter for sphere of equivalent volume
g = gravitational acceleration
L = characteristic length
L_o = test section width
R_{eq} = radius for sphere of equivalent volume
V = characteristic velocity
V_b = vertical velocity of bubble
$V_{w,l}$ = local vertical water velocity
$V_{b,r}$ = $V_b - V_{w,l}$ = relative bubble velocity

$$V_{w,mean} = \text{bulk water velocity} = \frac{1}{A}\int_A V_{w,l}\, dA$$

μ = dynamic viscosity of the liquid
ρ = liquid density
$\Delta\rho$ = density difference of the outer and inner fluids of the bubble
σ = interfacial or surface tension

$$\overline{C_D} = \text{drag coefficient} = \frac{4}{3}\frac{\Delta\rho}{\rho}\frac{g\,D_{eq}}{V_{b,r}^2}$$

$$N_{Eo} = \text{Eötvös number} = \frac{\Delta\rho\, g\, D_{eq}^2}{\sigma}$$

$$N_{Fr_{b,r}} = \text{Froude number} = \frac{V_{b,r}^2}{g\,D_{eq}}$$

$$N_{Re_{b,r}} = \text{relative bubble Reynolds number} = \frac{\rho\, D_{eq}\, V_{b,r}}{\mu}$$

$$N_{Re_s} = \text{system Reynolds number} = \frac{\rho\, L_o\, V_{w,mean}}{\mu}$$

$$N_{We_{b,r}} = \text{Weber number} = \frac{\rho\, D_{eq}\, V_{b,r}^2}{\sigma}$$

LITERATURE CITED

1. Baker, J. L. L., and B. T. Chao, *ME Tech. Rept. 1069-1*, University of Illinois, Urbana, Illinois (1963).
2. Allen, H. S., *Phil. Mag.*, **50**, 323, 519 (1900).
3. Miyagi, O., *ibid.*, 112; *Tohoku Imperial University Tech. Rept.*, **5**, 135 (1925).
4. Davies, R. M., and G. Taylor, *Proc. Roy. Soc. (London)*, **A200**, 375 (1950).
5. Peebles, F. N., and H. J. Garber, *Chem. Eng. Progr.*, **49**, 88 (1953).
6. Haberman, W. L., and R. K. Morton, *David Taylor Model Basin Report No. 802* (1953); *Trans. Am. Soc. Civil Engrs.*, **121**, 227 (1956).
7. Bloomfield, M., W. N. McElroy, and R. E. Skinner, *NAA-sr-2551*, Phys. and Math., Office of Technical Services, Washington D. C. (1958).
8. Monod, P., Centre d'Etudes nucl. Seclay, Ser. Bibliograph in French (1962).
9. Harmathy, T. Z., *A.I.Ch.E. Journal*, **6**, 281 (1960).
10. Hu, S., and R. C. Kintner, *ibid.*, **1**, 42 (1955).
11. McFadden, P. W., and P. Grassman, *Int. J. Heat Mass Transfer*, **5**, 169 (1962).
12. White, E. T., and R. H. Beardmore, *Chem. Eng. Sci.*, **17**, 351 (1962).
13. Wallis, G. B., *Int. Dev. Heat Transfer*, University of Colorado, p. 319 (1961).
14. Nicklin, D. J., *Chem. Eng. Sci.*, **17**, 693 (1962).
15. Garner, F. H., and D. Hammerton, *ibid.*, **3**, 1 (1954).
16. Birkhoff, G., and E. H. Zarantonello, "Jets, Wakes, and Cavities," Chap. 11, Academic Press, New York (1957).
17. Rosenberg, B., *David Taylor Model Basin Report No. 727* (1950).
18. Roll, J. B., Ph.D. thesis, Purdue University, Lafayette, Indiana (1962).

Manuscript received November 11, 1963; revision received November 13, 1964; paper accepted November 13, 1964.